Interactions of Organosilanes with Fibrinogen and their Influence on Muscle Cells Proliferation in 3D Fibrin Hydrogels

Kun Wang,† *Léa Trichet,* † *Clément Rieu,* † *Cécile Peccate,*‡ *Gaëlle Pembouong,*¥ *Laurent Bouteiller,* ¥ *Thibaud Coradin*†,*

† Sorbonne Université, CNRS, Laboratoire de Chimie de la Matière Condensée de Paris, 75005 Paris, France.

‡Sorbonne Université, Inserm UMRS974, Association Institut de Myologie, Centre de Recherche en Myologie, 75013 Paris, France.

¥ Sorbonne Université, CNRS, Institut Parisien de Chimie Moléculaire, 75005 Paris, France.

ABSTRACT: Silanization of biomacromolecules has emerged as a fruitful approach to prepare hybrid bio-hydrogels. However, very little is known about interactions between organosilanes and biopolymers in solution. Here we focused on fibrin, a protein of interest in the biomedical field, whose self-assembly process and resulting gel structure are highly sensitive to experimental conditions. Three main silanes were selected to decipher the relative influence of the silanol groups and organic functions. Whereas no protein denaturation was observed, silanes bearing hydrophobic groups had a surfactant-like behavior and could improve the dispersion of fibrinogen molecules, impacting on gel formation kinetics and rheological properties. 3D cultures of myoblasts evidenced that organosilanes could promote or impede cell proliferation, suggesting interactions of silanols with fibrin. These results demonstrate that the two sides of the coin of organosilanes reactivity are relevant at different stages of fibrin gel formation and must be considered for future development of hybrid biomaterials.

Keywords: fibrin, organosilane, hydrogels, myoblasts

Introduction

Fibrin is the major proteinaceous actor of the coagulation process.[1] Upon occurrence of a vascular injury, its precursor form, fibrinogen, is converted into fibrin under the action of the thrombin enzyme.[2-4] This conversion occurs in two steps, corresponding to the successive cleavage of two peptides (fibrinopeptides FpA and FpB) located in the central E region of the protein.[5-7] Removal of FpA enables intermolecular interactions between the E region and the two distal D regions to form protofibrils. Only after cleavage of FpB are fibrin molecules *per se* obtained, which then self-assemble into fibrils and fibers to form a protein mesh, or clot, incorporating aggregated platelets as well as red blood cells.[8]

Other proteins, such as plasmin and factor XIII, regulate the stability/degradation of the fibrin network *in vivo*.[9] However, they are not required to form fibrin gels *in vitro* : simple mixing of fibrinogen and thrombin solutions near neutral pH leads to clot-like networks.[10] Protein and enzyme concentration, temperature, pH, ionic strength and calcium amount are parameters allowing to tune the kinetics of the self-assembly and the structure of the final gel.[11-15] Fibrin processing into 3D-printed scaffolds, threads, microbeads and nanoparticles has already been described.[16-19] Such a versatility, combined with the high bioactivity of fibrin, opens many biomedical applications for these gels.[20-25] However, so far, their clinical use has been restricted to a glue form exhibiting sealing, adhesive and homeostatic properties.[26]

Fibrin networks usually exhibit high extensibility but relatively moderate elastic modulus at low stress, as well as fast biodegradation rates *in vivo*, which limit their use as biomaterials.[27-30] Both can be improved by tuning protein/thrombin concentration, using biological or chemical cross-linkers or forming (nano)composites.[31-36] One interesting alternative to strengthen and stabilize bio-hydrogels that recently emerged is based on silanized biomacromolecules.[37] In

several examples, such as gelatin,[38] alginate,[39] chitosan,[40] or hydroxypropolymethylcellulose,[41] organosilanes R'-Si(OR)$_3$ are used, where the organic function R' is selected to interact with the biomacromolecule chains and the alkoxysilane groups can be involved in the formation of a siloxane Si-O-Si network. The later process offers the possibility to obtain hybrid materials that take advantage of the chemical and mechanical properties of the silica network.[38] Moreover, because the silanol condensation is slow in acidic or very alkaline conditions and fast near neutral pH, it allows the development of injectable formulations.[41] However the picture is not that simple and the reactivity of both the silanol and organic groups must be taken into account in a balanced manner to fully predict the interactions of organosilanes with biopolymers.[42,43]

When focusing on functional proteins, an important question is whether organosilanes may induce their denaturation. This question has been addressed for silanized surfaces,[44] as well as within silica-based hosts.[45] However, in such cases, the organosilane is not present in an isolated molecular form but is part of a condensed phase. Interactions between specific biomolecules and soluble silica sources have been studied in the field of biomimetic silica formation,[46] but most of these works focused on the influence of these molecules on silane reactivity rather than silane influence on protein structure. One noticeable exception is type I collagen for which several studies devoted to the effect of silica sources on its self-assembly are available.[47] These works evidenced that, at low concentrations, silicic acid can promote collagen fibrillogenesis, due to a modification of the protein hydration and intra-fibrillar hydrogen bond network.[48] In contrast, at higher concentrations where silanol condensation occurs, fibrillogenesis was hindered, due to interactions between silica oligomers and collagen that are detrimental to protein-protein interactions.

Therefore, identifying and understanding the possible influence of organosilanes on fibrin fibrillogenesis is of major importance before developing hybrid silica-fibrin biomaterials. For this purpose, we selected here several precursors exhibiting distinct organic functions and studied their impact on fibrin self-assembly. These silanes were used at concentrations below the solubility limit of silica to limit their condensation and identify relevant interactions at the molecular scale. Particular attention was paid to distinguish between the three stages of the process, thrombin-induced conversion of fibrinogen to fibrin, fibrin self-assembly and fibrin gel maturation, that were studied by a combination of optical, thermal and rheological analyses. Moreover, the resulting gels were used for the 3D culture of a myoblast cell line as such or under differentiation conditions, allowing to enlighten the biological impact of organosilane-fibrin(ogen) interactions.

Experimental Section

Fibrinogen Solutions and Fibrin Gel Preparation. Fibrinogen (fbg) was purchased from EMD Millipore. The pure fibrinogen solution (6 $mg.mL^{-1}$) was prepared by diluting 150 µL of the stock solution (40 $mg.mL^{-1}$ reconstituted in water under vortexing from a lyophilized 20 mM sodium citrate-HCl solution and stored at 4°C) in 849.5 µL of the citrate buffer solution under vortexing. Pure fibrin gels were prepared by mixing the pure fibrinogen solution with 0.5 µL thrombin (bovine plasma from Sigma, dissolved to 200 $U.mL^{-1}$ in PBS) to form a 1 mL fibrin gel.

The silanes used in this work included methyltriethoxysilane (mt), tetraethoxysilane (teos), 3-aminopropyl-triethoxysilane (am), ethyltriethoxysilane (etes) and 3-(2,4-dinitrophenylamino)-propyltriethoxysilane (dnpt), obtained from Sigma Aldrich (**Figure 1**).

They were prepared as pre-hydrolyzed 10 mM solutions by dissolution in the distilled water and stirring overnight at room temperature in HCl 10^{-2} M (pH = 2). Further dissolution to 1, 0.1 and 0.01 mM was performed in citrate buffer (pH 7.2). Fibrinogen-silane solutions were prepared by mixing 150 µL of the fibrinogen stock solution with 749.5 µL of citrate buffer and adding 100 µL of the different pre-hydrolyzed silane solutions, with a final pH of 7.2. Fibrin-silane gels were obtained by mixing the fibrinogen-silane solutions with 0.5 µL thrombin (200 $U.mL^{-1}$). Similar procedures were followed to study the effect of hexanol (Fluka) on fibrinogen and fibrin gels.

Kinetics Study by UV-Visible Spectrophotometry. Fibrinogen and fibrinogen-silane solutions (999.5 µL) were added into a 1mL cuvette and the absorbance at λ = 400 nm recorded using the Time Drive mode of the UVIKON XS equipment with a scan rate of 15 spectra per minute. After 30 s, the solution was transferred to an Eppendorf tube, 0.5 µL of thrombin solution was added, the mixture shaken with a vortex for 15 s before being transferred to a new cuvette. Care was taken to standardize the whole duration of this step to 30 s. The absorbance was then recorded for the next 29 minutes. Each experiment was performed in triplicate.

Circular Dichroism Measurements. Circular Dichroism (CD) measurements for the pure and mixed fibrinogen solutions without thrombin were recorded in the 185-300 nm range in Quartz cuvettes with an optical pass length of 0.01 mm on a JASCO J810 spectropolarimeter combined with a Peltier temperature controller set at 37°C. Each experiment was performed five times.

Nano Differential Scanning Calorimetry. The pure and mixed fibrinogen solutions without thrombin were studied using a N-DSCIII instrument between 20 °C and 110°C at a heating rate of $1°C.min^{-1}$. The reference cell was filled with the citrate buffer and the sample cell filled with

0.3 mL of sample solution. The capillary cells were not capped, and a constant pressure of 5.10^5 Pa was applied. Each experiment was conducted in triplicate.

Dynamic Light Scattering. The hydrodynamic radius of fibrinogen and fibrinogen aggregates in pure and mixed solutions was measured by dynamic light scattering (Zetasizer Nano ZSE, MALVERN) at 37 °C and after heating for 10 min at 95°C. The type of cell was DTS0012 and the measurement angle was 90°.

Rheological Monitoring of Gel Formation. The rheological analysis of gel formation was performed using a MCR 302 rheometer from Anton Paar. Pure and mixed fibrinogen solutions with added thrombin were placed on the sample holder fitted with cone and plate geometry with a fixed gap width. Gelling at 37°C was dynamically tested on a rheometer plate at constant amplitude and angular frequency ($\gamma = 0.1\%$, $\omega = 0.5$ rad.s^{-1}).

Study of dye retention. A mixed solution of 3-(2, 4-dinitrophenylamino) propyl-triethoxysilane (dnpt, 1 mM) with fibrinogen was prepared as as described above for the other silanes and then 0.5 µL of thrombin was added to form 1 mL gels. After 12 h, 1 mL of phosphate buffered saline (PBS) was placed on the gel surface. After 1 h, the supernatant was withdrawn and its UV-vis spectra was recorded between 180 nm and 580 nm. Then 1mL of fresh PBS was added and left for 24 h before recording the UV-vis spectra. As reference, the UV-vis spectra of pre-hydrolyzed dnpt solutions in the 0.1 mM-1 mM concentration range were also recorded.

Cell Culture and Encapsulation in Fibrin Gels. C2C12 cells were grown in DMEM medium supplemented with 20% fetal bovine serum and 1% penicillin/streptomycin at 37°C in a humidified incubator with 5% CO_2, and passaged every 2 days. Pure and mixed fibrinogen solutions were mixed with 1mL of cell suspension at passage 12 containing 40000 C2C12 cells in a 12-well plate and then thrombin was added to form gels. The final concentrations of

fibrinogen and silanes were 6 mg.mL^{-1} and 0.01mM, respectively. After the formation of gels, 1 mL of growth medium was added on the top of the gels. After 4, 6, 8 and 10 days, the medium was discarded and 800 µL of the Alamar Blue reagent (0.1 mg.mL^{-1} from ThermoFisher) was added to well. After incubation at 37 °C for 4 h, the fluorescence emission at 585 nm was used to calculate the percentage of reduction of Alamar Blue. Cytotoxicity tests were performed using the Alamar Blue method on 2D cultures of C2C12 cells kept in contact for 6 days with 0.01 mM solutions of selected pre-hydrolyzed silanes.

Confocal Laser Scanning Microscopy of differentiated C2C12 cells. C2C12 were encapsulated in fibrin and fibrin-silane gels following the above described protocol. After the formation of gels, 1 mL of growth medium was added on the top of the gels and changed after 2 days. After 4 days, it was replaced by 1 mL of differentiation medium (DMEM supplemented with 2% donor equine serum and 1% penicillin/streptomycin). After 7 additional days, cells were fixed with 4% PFA and permeabilized with 0.5 % Triton X-100 for 15 min. After several rinsing with PBS solution, actin filaments were stained with Alexa Fluor 488 phalloidin and nuclei with 4',6'-Diamidino-2-phenylindole (DAPI) solution. Gels were imaged with a Confocal Laser Scanning Microscope (CLSM, inverted Nikon Ti equipment). Digital images were acquired with a CoolSNAP HQ2 camera using Metamorph software and processed using Image J software. Staining of myosin heavy chain in differentiated C2C12 was performed with MF-20 hybridoma mouse IgG2B primary antibody and Alexa Fluor 546 goat anti-mouse IgG2B secondary antibody (Invitrogen). Gels were imaged on a Confocal Laser Scanning Microscope (Zeiss LSM 710). The images were processed and analyzed using Image J software. The index fusion was estimated on at least 2 different images for each type of samples. The number of nuclei was calculated by means of Analyze particles command after image binarization. A minimum of 150 nuclei (with

an average of 387 nuclei) were taken into account for each type of samples to make the calculations.

Statistical Analyses. Analysis of data was performed through variance analysis (ANOVA) and the mean comparisons were done by Duncan's multiple range tests. Statistical analysis was performed using the Statistical Package for Social Sciences (SPSS for Windows, SPSS Inc.,Chicago, IL, USA). Data were presented as means ± standard deviation and a probability value of $P < 0.05$ was considered significant. The smallest measured value is marked with letter a and statistically-different measures of increasing value are marked with following letters in alphabetical order.

Results

Influence of Organosilanes on Fibrin Gel Formation. Initially we selected three different silanes that were pre-hydrolyzed in acidic media: tetraethoxysilane (teos) that is converted into silicic acid $Si(OH)_4$, methyltriethoxysilane (mt) yielding to CH_3-$Si(OH)_3$ and aminopropyltriethoxysilane (am) forming NH_2-$(CH_2)_3$-$Si(OH)_3$ (**Figure 1**). The use of teos should permit to evaluate the interaction of silanol Si-OH group with fibrinogen and/or fibrin whereas mt and am have additional hydrophobic and cationic moieties, respectively. The maximum concentration of silane was fixed to 1 mM (*i.e.* below the silica solubility) to limit their oligomerization/condensation.

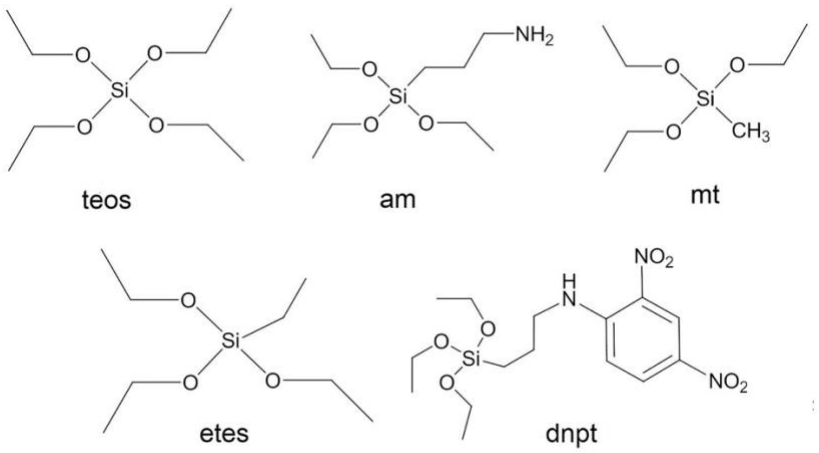

Figure 1. Chemical formula of the different silanes used in this work.

In a first step, the influence of silane addition on fibrinogen solutions in the presence of thrombin at pH 7.3 was followed by UV-visible spectrophotometry measurements at λ = 400 nm, *i.e.* turbidity curves. A typical curve for fibrin gels begins with a lag phase where the absorbance remains constant corresponding to the cleavage of the FpA peptide of fibrinogen by thrombin (**Figure 2**). Then absorbance increases rapidly and follows a sigmoidal variation until reaching a plateau. The time point where the curve starts to increase is often termed the "clotting time" and corresponds to the cleavage of the FpB peptide of fibrinogen, which converts it into fibrin molecules that can self-assemble into fibrils of increasing size.[12] In this study, fibrinogen and thrombin concentrations were adjusted to 6 $mg.mL^{-1}$ and 0.1 $U.mL^{-1}$, respectively, to obtain a short but accurately measurable clotting time and a final absorbance that would remain reliably recorded by the spectrophotometer even if silane addition would increase it by 50 % (Supporting Information, **Figure S1**).

As shown in **Figure 2**, for fibrinogen without added silane (dark lines), the clotting time is 2.5 min and the maximum absorbance is ca. 2.3. After silane addition, no clear modification of

the clotting time could be observed but changes in initial slope and maximum absorbance were evidenced**.** Based on triplicate experiments, adding teos at 0.01 mM, 0.1 mM and 1 mM induced a clear increase in the initial slope of the curve and a small increase on the final absorbance (**Figure 2(a)**). A very similar evolution was observed upon addition of am (**Figure 2(b)**). However when mt was added, it was noticed a decrease in both slope value and maximum absorbance at 0.01 mM, an increase of both parameters at 1 mM and no clear variation at 0.1 mM (**Figure 2(c)**). Comparison of curves obtained at a fixed silane concentration of 1 mM enlightens the difference of mt addition over teos and am (**Figure 2(d)**) and Supporting Information, **Figure S2)**. Noticeably, it was checked that addition of equivalent amounts of ethanol, that may have remained in the silane hydrolysis solution, did not modify fibrin self-assembly (Supporting Information, **Figure S3**). Moreover, control experiments performed in the absence of fibrinogen show no contribution of silanes to the UV-vis curves (Supporting Information, **Figure S3**). Altogether teos and am had similar impact on the maximum absorbance and slope while mt had a statistically different influence on both parameters at the lowest investigated concentration (**Figure 2(e),(f)**).

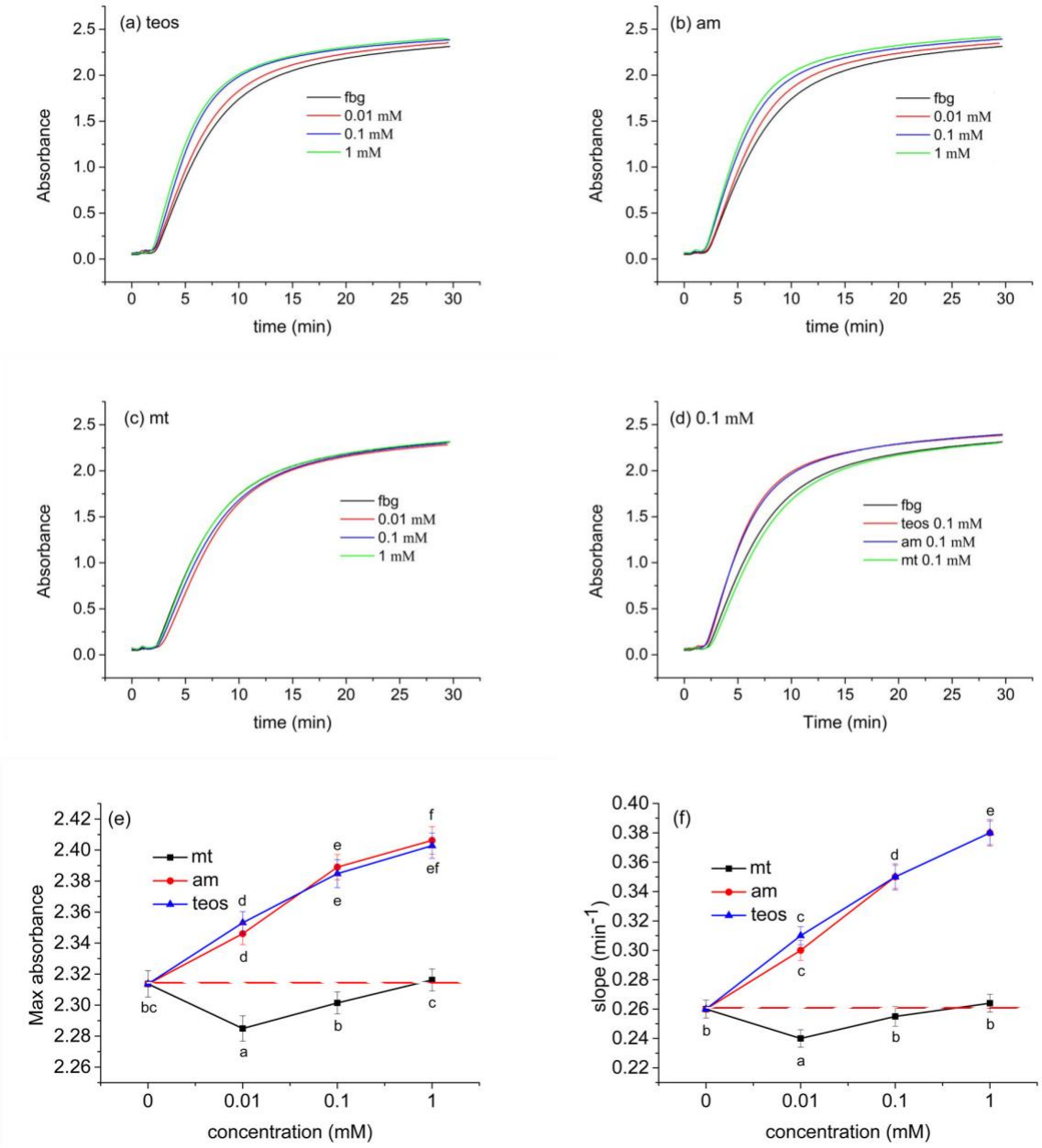

Figure 2. (a-d) Variation of absorbance at λ = 400 nm as a function of time of fibrinogen solutions after thrombin addition in the presence of (a) teos, (b) am and (c) mt at different concentrations and (d) in the presence of the three silanes at 0.1 mM. Dark lines correspond to pure fibrinogen solutions (fbg). All experiments were made in triplicates and the curves show the resulting average data. (e-f) Variation of (e) maximum absorbance and (f) initial slope of the

absorbance curves with silane nature and concentration. Dashed lines correspond to the fibrinogen reference. Error bars indicate standard deviation. Different letters correspond to statistically-different values ($P < 0.05$) as determined by ANOVA with Duncan tests.

The fact that no statistical difference was found between the clotting times measured in the presence of silanes (Supporting Information, **Figure S4**) indicates that these molecules do not interfere with the thrombin activity. It was checked that incubation of silanes with thrombin before fibrinogen addition led to the same UV-vis curves (Supporting Information, **Figure S5**). In contrast statistically-significant variations in slope and maximum absorbance (**Figure 2(e)-(f)**) suggests that they could modify the kinetics of self-assembly and/or the size of the fibrin fibrils. A first hypothesis was that the silanes could interact with the fibrin molecules. To check this, the silanes were added at a 1 mM concentration 5 min after the clotting time. As seen on Supplementary Information, **Figure S6**, none of the silanes had a clear effect on fibrin fibrillogenesis in these conditions of delayed addition. This implies that they mainly interact with the fibrinogen molecule.

Interactions of Organosilanes with Fibrinogen. Circular Dichroism was thus used to check any effect of silanes on fibrinogen conformation, in the absence of thrombin. As shown in **Figure 3**, the CD spectra of pure fibrinogen shows three major bands, one positive at $\lambda_1 = 190$ nm and two negative at $\lambda_2 = 209$ nm and $\lambda_3 = 220$ nm. A first observation of the spectra obtained at different concentrations of the three silanes (**Figure 3(a)-(c)**) indicates no major variation in their shape but rather in the relative intensity of the first peak compared to the two others. The peaks intensity I_n were therefore measured and ratio I_2/I_1 and I_2/I_3 were calculated. As shown on **Figure 3(d)**, compared to pure fibrinogen, I_2/I_1 was most significantly increased for mt at 0.01

mM and 0.1 mM and, to a lesser extent, for mt at 1 mM. In contrast, although some minor modification could be noticed in the 200-220 nm range, no significant variation was obtained for I_2/I_3 whatever the added silane or its concentration (Supplementary Information, **Figure S7**). It has been established that the CD spectra of fibrinogen is dominated by the signal of the α-helix conformation.[49] Antiparallel β-sheet contributes positively to I_1 and negatively to I_2 and I_3, β-turn conformation negatively to I_1 and positively to I_2 and random coil structure mostly negatively to I_1.[50] Therefore an increase in I_2/I_1 with no variation of I_2/I_3, as observed for mt, would point for a decrease of the contribution of the random coil with no other major conformational modification.

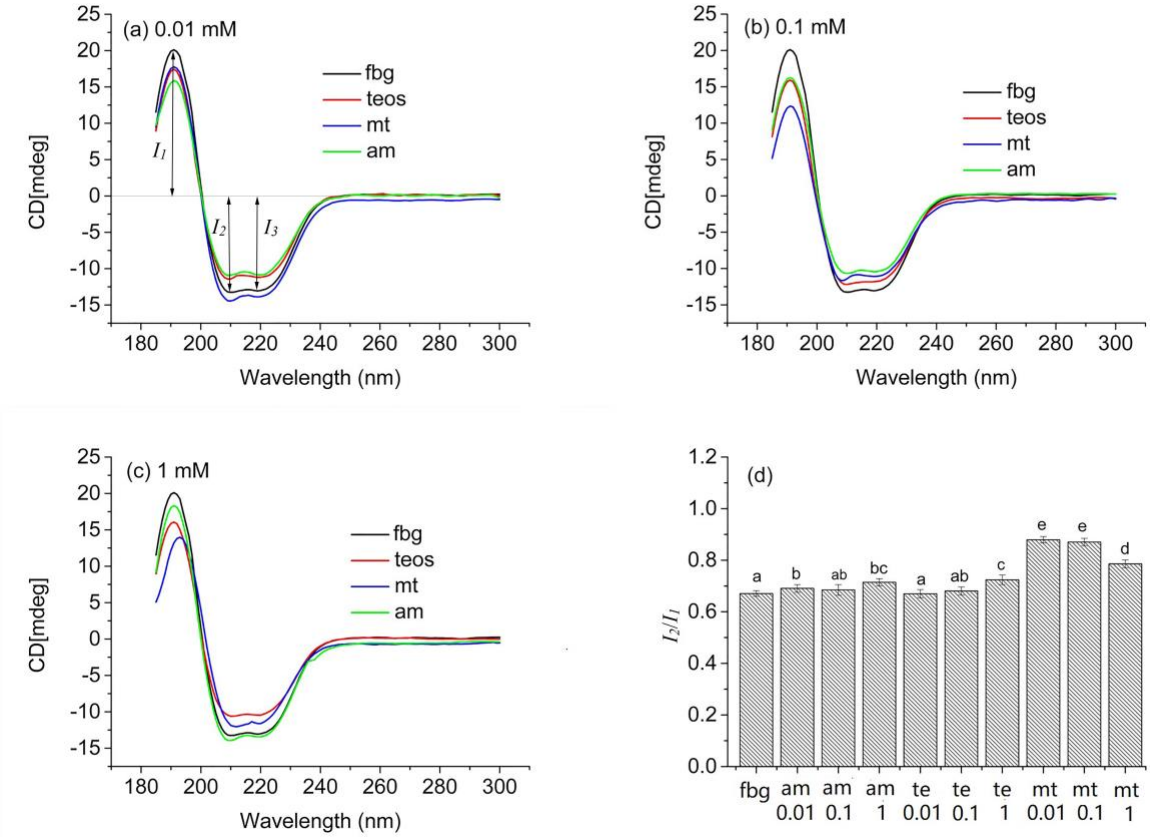

Figure 3. CD spectra of fibrinogen (fbg) and with the three silanes at (a) 0.01 mM, (b) 0.1 mM and (c) 1 mM; (d) Calculated ratio of intensity of peak 2 over peak 1 (I_2/I_1) for the different samples. Different letters correspond to statistically-different values ($P < 0.05$) as determined by ANOVA with Duncan tests.

In order to obtain further information on the interaction between fibrinogen and silanes, nano-Differential Scanning Calorimetry (nanoDSC) experiments were performed. For pure fibrinogen, two peaks at 52 ± 0.2 °C and 95° ± 0.5 °C were recorded corresponding to the melting temperature of the D region and denaturation of the E region of fibrinogen, respectively (**Figure 4**).[51,52] In the presence of teos, the peak temperatures were not modified but a decrease in intensity of the signal above 100°C was noticed at 1 mM (**Figure 4(a)**). For mt, this part of the nanoDSC curve increased in intensity with the silane content (**Figure 4(b)**). A similar trend was obtained for am (**Figure 4(c)**) although to a smaller extent than for mt (see comparison on **Figure 4(d)**).

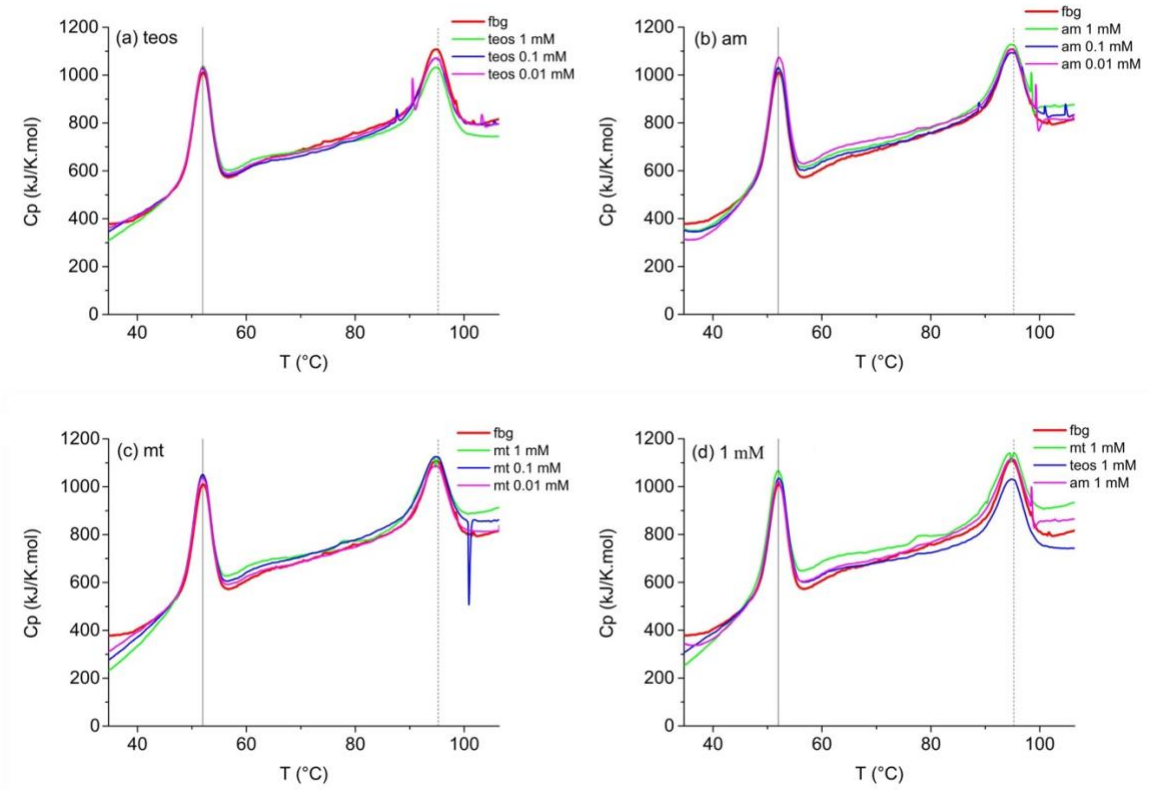

Figure 4. Nano-DSC thermograms of fibrinogen solutions in the presence of (a) teos, (b) am and (c) mt at different concentrations and (d) in the presence of the three silanes at 1 mM. Red lines correspond to pure fibrinogen solutions (fbg). Reference was citrate buffer (pH = 7.2).

Based on the literature, we hypothesized that such variations of heat capacity above 100°C could be associated to modification of the aggregation state of the fibrinogen molecules.[49,53] Fibrinogen-silane mixtures were therefore studied by Dynamic Light Scattering before and after heating (**Figure 5**). For the initial solution, pure fibrinogen leads to an average hydrodynamic radius of 20 nm, in agreement with the literature data.[54] This value was not significantly modified upon mt addition but increased when teos or am solutions of increasing concentrations were added. Similar trends were observed after heating: while pure fibrinogen and fibrinogen-mt aggregates had comparable dimensions (*ca*. 700 nm), those obtained in the

presence of am and teos were much larger, especially at the highest silane concentration (up to *ca*. 1600 nm).

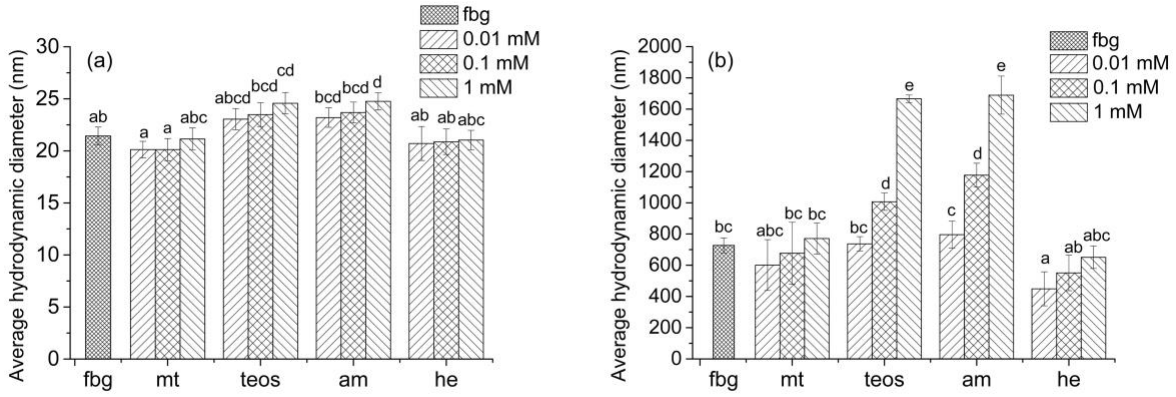

Figure 5. Average hydrodynamic diameter of fibrinogen in citrate buffer (pH 7.2) in the presence of silanes and hexanol (he) (a) before and (b) after 10 minutes heating at 95 °C. Different letters correspond to statistically-different values ($P < 0.05$) as determined by ANOVA with Duncan tests.

At this stage, it is therefore possible to assume that mt can interact with fibrinogen and decrease its tendency to aggregate without modifying its conformation nor its ability to interact with thrombin. Such an ability of mt to disperse fibrinogen would also be consistent with the lower values of slope and maximum absorbance recorded by UV-vis. Since neither teos nor am show a similar effect, we hypothesized that the hydrophobic character of the methyl moiety of CH_3-$Si(OH)_3$ should be responsible for these properties. More specifically, hydrolyzed mt silanes may behave as amphiphilic molecules that can favor the dispersion of certain proteins.

To check this hypothesis, we first selected another hydrophobic silane, ethyltriethoxysilane (etes) (**Figure 1**). CD analysis showed again an increase of the I_2/I_1 ratio

compared to pure fibrinogen, especially at low silane content, while I_2/I_3 was not significantly modified (**Figure 6** and Supplementary Information, **Figure S8**). In a second step we evaluated the effect of hexanol as a relatively soluble organic hydrophobic molecule, with similar results on the CD spectra (**Figure 6)**. Hexanol was also tested for DLS experiments (**Figure 5**) and showed a very similar capacity to mt to favor fibrinogen dispersion before heating and limit its aggregation after heating.

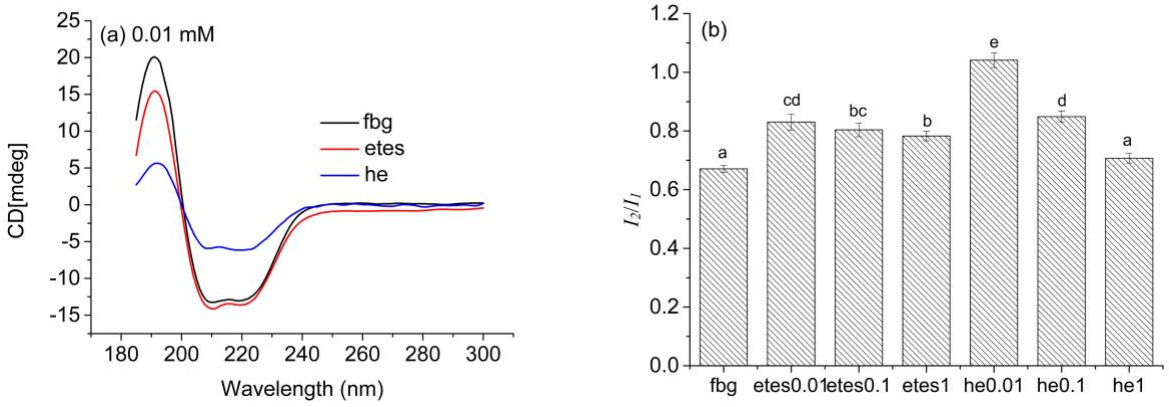

Figure 6. (a) CD spectra of fibrinogen as such (fbg) and with etes and hexanol (he) at 0.01 mM, (b) Calculated ratio of intensity of peak 2 over peak 1 (I_2/I_1) for the different samples. Different letters correspond to statistically-different values ($P < 0.05$) as determined by ANOVA with Duncan tests.

Influence of Organosilanes on Fibrin Gel Properties. We then turned our attention on the properties of the resulting fibrin gels. First their rheological behavior was studied. It was observed that, in the previous conditions of studies at 25°C, the storage modulus value *G'* for pure fibrin gels was not reached after *ca*. 2 days (not shown). It is worth noticing that such a delay contrasts with the UV-vis data where a plateau was reached within less than one hour, suggesting that whereas a physical network is established rapidly after the clotting time, it

continues to evolve significantly with time. To reach reasonable experimental conditions, following experiments were performed at a temperature of 37°C in order to speed up the gelation process and get closer to in vivo conditions. Pure fibrinogen reaches a plateau at *G'* = 175 Pa after 7 h (**Figure 7**). With teos at 0.01 mM, the initial slope was similar but the plateau was reached after a longer period (12 h) and the *G'* value was higher, *ca*. 240 Pa (**Figure 7(a)**). With am, the plateau was reached slightly sooner than for teos (10 h) but *G'* was also greater, *ca*. 270 Pa. For mt at 0.01 mM, the plateau took much longer time to be reached (17 h) and *G'* was also higher than for fibrinogen but smaller than for the other silanes. Major differences between 0.01 mM and 1 mM silane concentrations were a slight increase in *G'* value for teos and a shorter time to reach plateau for mt (**Figure 7(b)**). The addition of etes has similar effect to mt addition while hexanol had no impact on the required time to reach the plateau but decreased the final *G'* value, especially at a 0.01 mM concentration (**Figure 7(c),(d)**). Variation of the loss modulus *G"* followed a similar trend to *G'* but with lower values, as expected for gels (Supplementary Information, **Figure S9**).

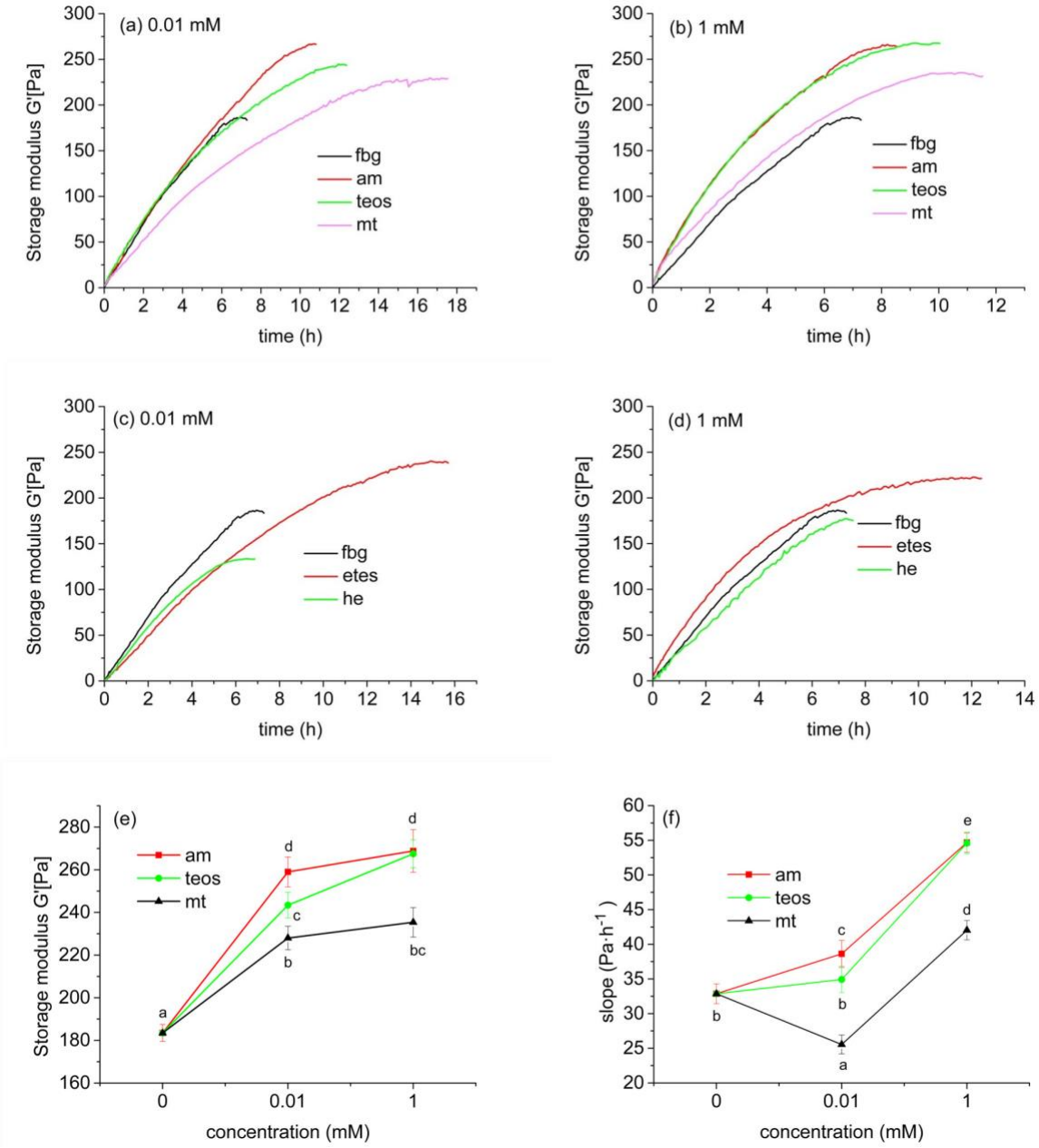

Figure 7. (a-d) Evolution of storage modulus *G'* of fibrin gels with time at 37°C in the presence of different silanes and hexanol at (a,c) 0.01 mM and (b,d) 1 mM. All experiments were made in triplicates and the curves show the resulting average data. (e-f) Variation of (e) maximum storage modulus and (f) initial slope of the rheological curves with silane nature and

concentration. Error bars indicate standard deviation. Different letters correspond to statistically-different values ($P < 0.05$) as determined by ANOVA with Duncan tests.

Altogether, all silanes increase *G'* values of fibrin gels to a small but statistically-different extent. The highest and lowest *G'* values were obtained for am and mt, respectively, at 0.1 mM with no significative further increase at 1 mM (**Figure 7(e)**). The reaction kinetics followed a similar trend to UV-vis data, with a statistically-significant decrease of the curve slope for mt at 0.01 mM and increase for am and teos at both concentrations, with a systematic increase of the time required to reach the plateau compared to fibrinogen (**Figure 7(f)**). The fact that hexanol decreases *G'* value and does not impact on the reaction kinetics suggests that the silanol groups born by the hydrolyzed silanes, and not the hydrophobic moieties, are mostly responsible for these modifications.

To clarify this point further, we used 3-(2, 4-dinitrophenylamino) propyl-triethoxysilane (dnpt), an organosilane bearing a fluorescent dye (**Figure 1**). Its pre-hydrolyzed form was added at a 1 mM concentration to the fibrinogen/thrombin solution and the gel was left to form over 12 h. Then it was covered with 1 mL of PBS and the fluorescence spectra of the supernatant was recorded after 1 h and 24 h and compared to pre-hydrolyzed dnpt solutions at various concentrations. As shown in Supplementary Information, **Figure S10**, *ca*. 1/10 of the dye was released after 1 h while, after 24 h, the dye concentration was below 0.25 mM. Therefore, taking into account the dilution effect that would lead to 0.5 mM dye in the supernatant if it had been fully released, more than one half of the initially introduced dnpt molecule remained trapped

within the gel. Since the dye moiety is not expected to form strong bonds with the protein, this result suggests that significant interactions exist between the fibrin network and silanol groups.

Finally, the impact of teos, am and mt on the ability of fibrin gels to act as 3D matrix for muscular cells growth was studied. For this purpose, C2C12 cells were encapsulated with fibrin and fibrin-silane gels in a DMEM medium supplemented with 20 % fetal bovine serum and their proliferation was followed by Alamar Blue test. As shown on **Figure 8**, cell population in pure fibrin gels slowly increased during 6 days and then more rapidly. Similar curves were obtained in the presence of silanes at 0.01 mM but after 8 days, the proliferation rate was statistically significantly higher in the presence of am than for pure fibrin and with added teos, whereas it was slightly but statistically smaller in the presence of mt. To rule out any cytotoxic effect of the silanes, their influence on C2C12 grown in 2D was studied, showing no significant difference with the silane-free control after 6 days (Supplementary Information**, Figure S11**).

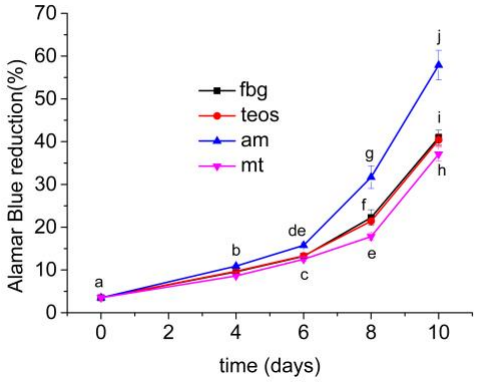

Figure 8. Evolution of C2C12 proliferation within fibrinogen and fibrinogen-silane gels as monitored by Alamar Blue test. Error bars indicate standard deviation. Different letters correspond to statistically-different values ($P<0.05$) as determined by ANOVA with Duncan tests.

In a step further, the ability of the different hydrogels to favor C2C12 differentiation was studied. For this purpose, cells were cultured for 4 days in the same serum-rich DMEM medium as previously and for 7 additional days in a low serum (2% donor equine serum)-DMEM medium. Cells embedded in pure fibrin gels and gels made of fibrin with mt or am showed a high proliferation capacity and formed large, disorganized tridimensional structures, whereas the cells did not adhere well in the gels made with teos (**Figure 9**).

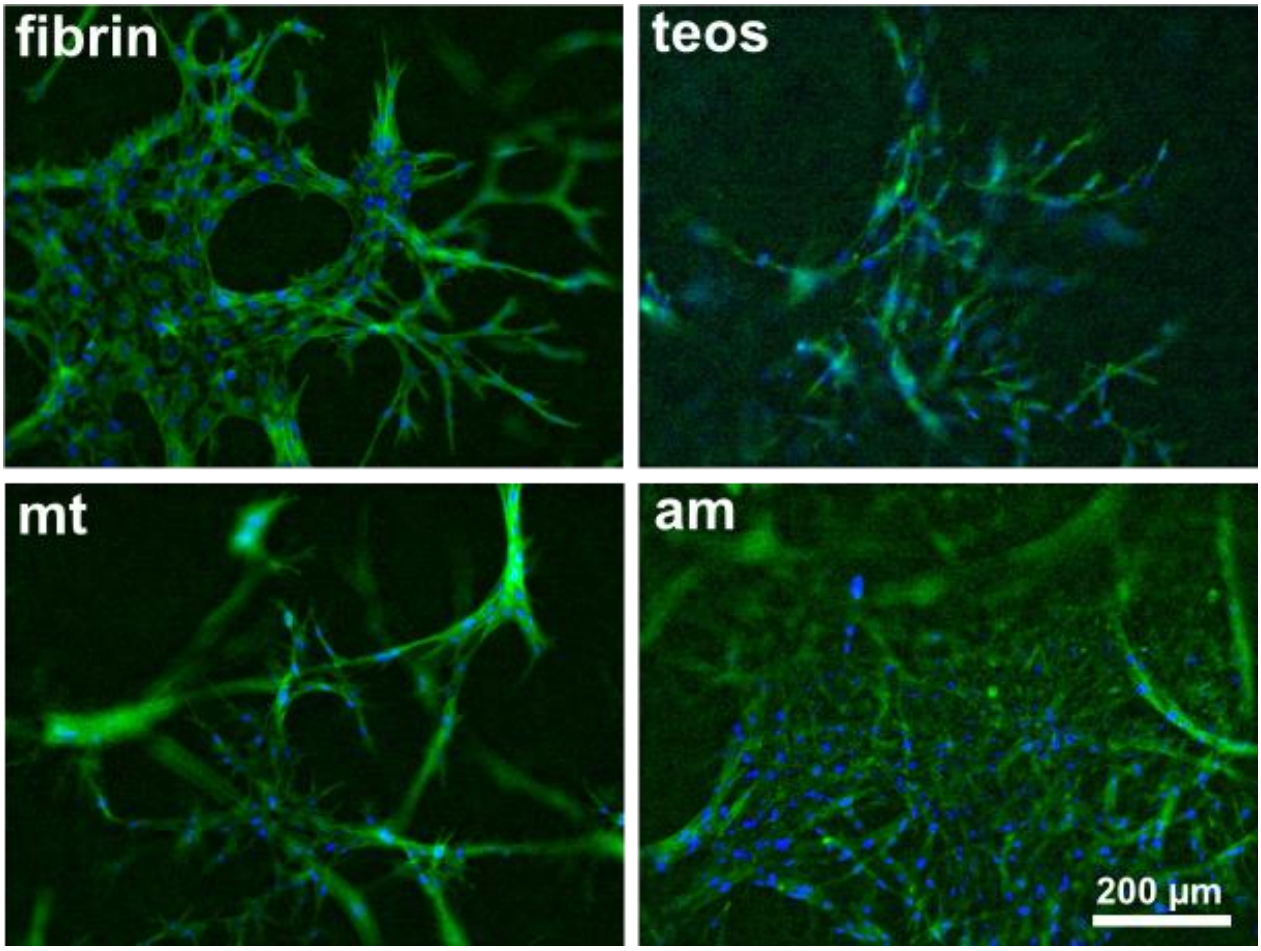

Figure 9. CSLM images of C2C12 cells cultured for 4 days in serum-rich and 7 days in low-serum DMEM within fibrin, fibrin-teos, fibrin-mt and fibrin-am hydrogels. (Blue: DAPI, green: Alexa Fluor 488 phalloidin)

In pure fibrin and fibrin plus mt the obtained structures appear mainly branched. The obtained networks seem to be more evenly distributed in the presence of mt compared to pure fibrin, with less cells being clustered. Formation of myotubes is clearly evidenced by MF20 positive staining (**Figure 10**). The estimated fusion index is similar for fibrin and fibrin plus am (29 and 26%, respectively). It is lower in the presence of teos (13%) and higher with mt (35%).

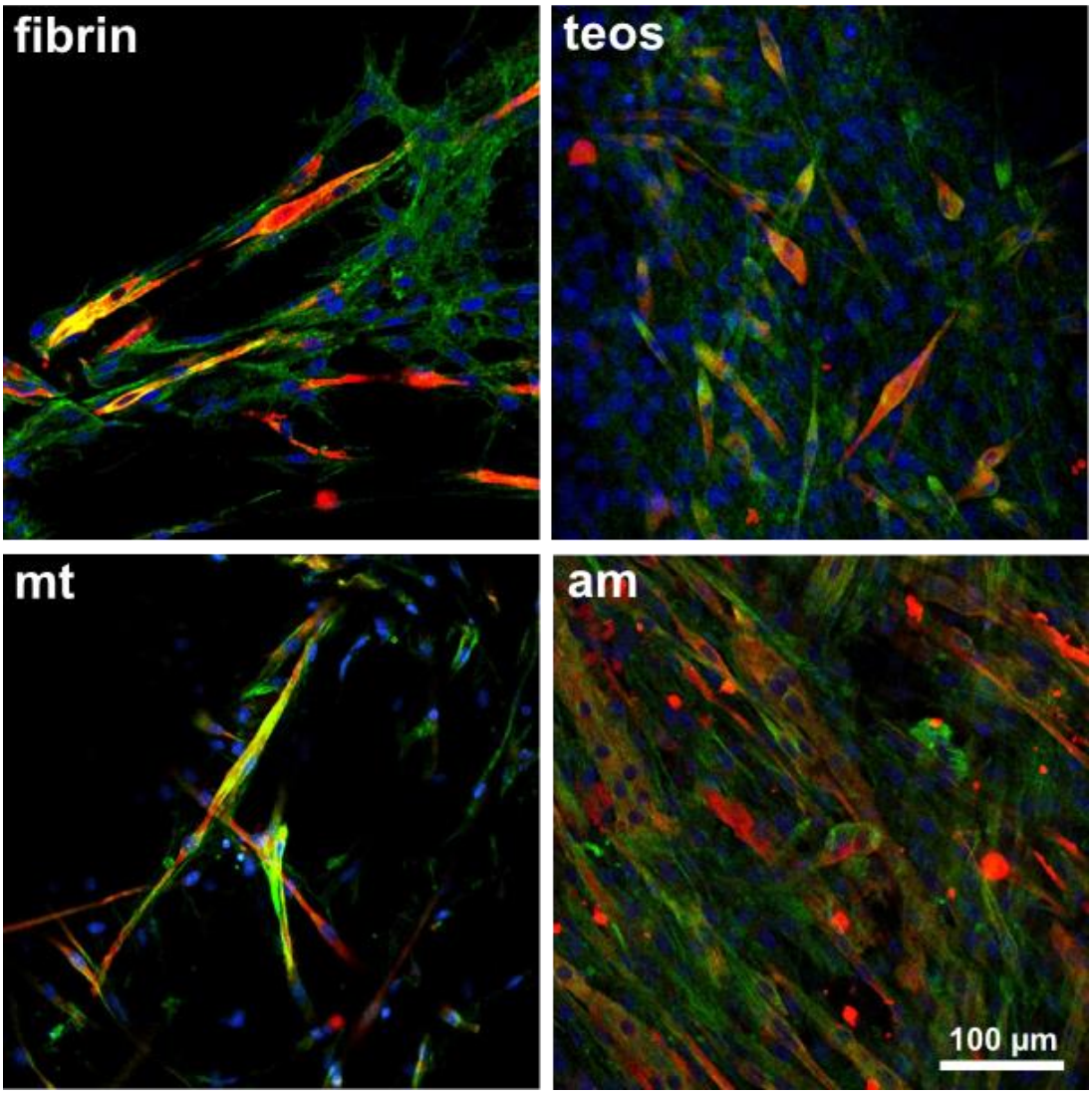

Figure 10. CSLM images of C2C12 cells cultured for 4 days in serum-rich and 7 days in low-serum DMEM within fibrin, fibrin-teos, fibrin-mt and fibrin-am hydrogels. (Blue: DAPI, green: actin, red: MF20)

Discussion

Here-gathered data demonstrate that organosilanes at low concentration (*i.e.* below the silica solubility limit) can influence the formation and properties of fibrin gels. To better discuss these results, it is important to consider three different stages: (i) the fibrinogen-to-fibrin conversion induced by thrombin, (ii) the self-assembly of fibrin and (iii) the maturation of the fibrin gel.

The first stage is itself occurring in two steps, corresponding to the successive cleavage of two peptides.[5] It is usually admitted that the first cleavage only leads to protofibrils whose dimensions are too small to induce light scattering at $\lambda = 400$ nm.[8] On the UV-visible absorbance curve, it corresponds to the initial domain with no change in intensity. When the second cleavage occurs, fibrin molecules are formed and can self-assemble into fibers, large enough to scatter light, which corresponds to the sharp increase in the diffusion/absorbance curve. The delay between thrombin addition to fibrinogen solutions and increase in absorbance, the clotting time, can therefore provide some information on the first step of the conversion process. Here, in all studied conditions, no significant variation in clotting time was measured. This indicates that the organosilanes do not significantly alter thrombin nor fibrinogen structure, at least at the proximity of the cleavage site. Along this line, CD spectra do not evidence specific modifications of the α-helix, β-sheet and β-turn content but only, in some cases, an increase in the contribution of the random coil structure. Accordingly, nano-DSC results do not show significant shifts in the melting temperature of the lateral D region nor in the denaturation temperature of the E region, where the FpA and FpB peptides are located.

However, despite the absence of significant modification of fibrinogen structure, the course of the UV-visible absorbance curve after the clotting time shows a clear dependence on

the nature and concentration of the silanes. The initial slope of the curve provides indication on the kinetics of the self-assembly process while the maximum absorbance should reflect the dimensions of the resulting fibers. In this regard, all silanes have a noticeable influence on both parameters, in a concentration-dependent manner. Importantly, when the silanes are added after the self-assembly process has started, they have no significant influence on the slope and maximum absorbance. This suggests that they do not interact with fibrin molecules in these conditions.

The most plausible explanation for these observations can be obtained from DLS data, and are supported by the nano-DSC variations obtained at high temperature. These suggest that the silanes can modify the state of aggregation of fibrinogen in the starting solution and that this modification has a clear impact on the protein dispersion after denaturation. Importantly, there is a good correlation between DLS and UV-vis data as silanes that increase fibrinogen aggregation state (teos, am) leads to larger slopes and maximum absorbance for fibrin gel formation, with a parallel trend when their concentration is increased. This would suggest that the self-assembly process is favored and larger fibers are formed when fibrinogen aggregation is higher. On the opposite, mt can decrease fibrinogen aggregation as well as slope and maximum absorbance, although to a small extent and only at very low concentration (0.01 mM).

To understand how organosilanes can modulate fibrinogen aggregation, it is important to compare their structure and reactivity. In UV-visible experiments, teos and am have a similar behavior, whatever their concentration. This is also true considering CD and DLS data. The only minor difference appears on the nano-DSC results where an increase in heat capacity is observed in the high temperature domain for am at 1 mM while a decrease is measured for teos at the same concentration. From a chemical point of view, hydrolyzed teos ($Si(OH)_4$) and am (NH_{3+}-C_3H_7-

$Si(OH)_3$) only differ by the propyl-ammonium group. Thus it can be suggested that the fibrinogen-aggregation ability of these silanes is mainly due to the silanol groups. As a matter of fact, it has already been shown that silicic acid at low concentration could favor the self-assembly of type I collagen proteins by modification of the inter-molecular hydrogen bond network as induced by the Si-OH groups.[48] This explanation would also stand here for teos. In the case of am, it seems that the presence of the propyl-ammonium chain has only a minor influence. It is worth noting that the isoelectric point of fibrinogen is *ca*. 5.5,[54] while our experiments are performed at pH 7.2 so that the protein is only slightly negatively charged. Therefore electrostatic interactions are very unlikely to play a major role in the observed phenomena.

In contrast, mt has a very distinct effect on fibrinogen, as evidenced by all techniques used here. Again, the methyl group of the CH_3-$Si(OH)_3$ hydrolyzed molecule must be responsible for this specific behavior, most likely due to its hydrophobic character. Interestingly, etes that bears an ethyl instead of a methyl group induces very similar modifications of the CD spectra of fibrinogen. Moreover, hexanol has a similar, but enhanced, effect on both CD spectra and fibrinogen aggregation state. These results can be interpreted in lights of the known interactions between protein and surfactants. Indeed hydrolyzed mt can be considered as an amphiphilic molecule with a neutral polar $Si(OH)_3$ head and apolar CH_3 tail. It has been shown that non-ionic surfactants below their critical micellar concentration (cmc) could prevent protein aggregation by a so-called chaperone effect.[55] In this situation, surfactant binding occurs in the hydrophobic domains of the protein, leading to minor structural modifications but, usually, not to protein denaturation. In our case, it would leave the silanol groups pointing from the proteins surface, making it more hydrophilic and therefore decreasing their tendency to aggregate.

However, when the surfactant concentration increases, and even if the cmc is not reached in the bulk solution, micellar objects can be formed because the accumulation of surfactants on the surface induces a higher local concentration that can drive their self-organization.[56] Such micelles are able to interact with large domains of the protein and to destabilize it, inducing unfolding and/or precipitation. Such an effect would explain why mt is more efficient to prevent fibrinogen aggregation at very low concentration.

Taken together, our data suggest that organosilanes can interact with fibrinogen, either favoring or limiting attractive intermolecular interactions. This impacts on the kinetics of fibrin self-assembly, modulating the fiber size. As pointed out earlier, whereas a maximum in absorbance is reached after a few minutes, rheological measurements show that further maturation of the gel network occurs up to *ca*. 7 h for pure fibrin and to 18 h in the presence of 0.01 mM mt. In the meantime, the final *G'* value also depends on the nature and concentration of added silane.

Importantly the initial slope of the UV-vis and rheological curves follow the same trend, *i.e*. compared to pure fibrinogen, it is larger in the presence of teos and am and smaller for mt at low concentration and it increases for all silanes at 1 mM. This is a good indication that the first period of the fibrin self-assembly process is not perturbed by the rheological measurements. Considering the *G'* values, they are also well-correlated with the maximum absorbance of the UV-vis curves for am and teos. However, for mt at 0.01 mM, the final *G'* value is larger than that of pure fibrin whereas its maximum absorbance was smaller. Looking at the corresponding curve, it is quite clear that while stabilization of fibrinogen-only gels occurs rapidly, the presence of mt slows down the process of reorganization of the fibrin network. Importantly, such a extended period of stabilization is observed for all other silanes in all conditions. This indicates

that in addition to the modification of interactions between fibrinogen molecules in the initial solution, organosilanes can also have some influence on the interactions between fibrin fibers on the long-term. In this context, it is interesting to note that hexanol do modify the final *G'* value but do not extend the time necessary to reach stabilization. This would suggest that the silanol groups play a key role in the organosilane interactions with fibers. As a matter of fact, experiments performed with the silane dye dnpt indicate that, after 24 h of contact with PBS, about half of this organosilane remains trapped within the fibrin gel. Whereas diffusional effects cannot be fully excluded, it can also support the existence of non-negligible interactions between silanols and fibers surface.

This assumption can also help to interpret the results obtained for C2C12 cells encapsulated within the different gels. In terms of proliferation, am has a distinct beneficial effect on the long-term. On the one hand, cytotoxicity tests indicated no detrimental effect of any of the three silanes over the growth period. On the other hand, the *G'* values for teos- and am-containing gels are similar so that any influence of the mechanical properties of the 3D matrix can be reasonably excluded. Thus the most plausible explanation lies in the presence of cationic ammonium groups that are known to favor adhesion of many cell types, as a consequence of am adsorption on the fibrin fiber surface. The observed influence of the different silanes appears clearly distinct for undifferentiated and differentiating cells, especially for teos and, to a lower extent, for am. The formation of myotubes requires that the precursor cells come into contact in order to differentiate and fuse and therefore depends on the possibility for these cells to contract and remodel the matrix.[57] The increase of fibrinogen aggregation as induced by teos and am might be detrimental to C2C12 interactions with fibrin and decrease their differentiation capability, thus explaining why cells seem to detach in the case of teos, whereas with am they go

on proliferating with no optimized differentiation when compared to fibrin alone. Along the same line, in the case of mt, the capacity of the cells to form highly branched tridimensional myotubes could arise from the increased fibrinogen dispersion originally induced by this silane.

Conclusions

Organosilanes at low concentration can influence the self-assembly process of fibrin and impact the physical and biological properties of the resulting gels. The main interactions at stake are occurring between fibrinogen and silanes, and highly depend on their organic functionality. However, once the gel has formed, a fraction of the silane molecules establishes significant interactions with the fibrin network, most probably via their silanol groups. These results are of major importance for the synthesis of silanized biopolymers and their use for biomaterial design. However, it is now necessary to extend this study to organosilanes bearing more reactive moieties, such as 3-glycidoxypropyl trimethoxysilane, and to increase their concentration to reach conditions where condensation can occur, both of which should enhance their impact on the structure and reactivity of biomacromolecules.

ASSOCIATED CONTENT

Supporting Information. Additional UV-vis, Circular Dichroism and rheological data; absorbance spectra of 3-(2, 4-Dinitrophenylamino) propyl-triethoxysilane in solution and in fibrin gels; cytotoxicity assays. The following files are available free of charge.

Supplementary data (PDF)

AUTHOR INFORMATION

Corresponding Author

*Phone: +33-1-44274018; E-mail: thibaud.coradin@sorbonne-universite.fr

Author Contributions

The manuscript was written through contributions of all authors. All authors have given approval to the final version of the manuscript.

Funding Sources

K.W. was funded by a China Scolarship Council PhD grant with additional support from the French state funds managed by the ANR within the Investissements d'Avenir program under reference ANR-11-IDEX-0004-02, and more specifically within the framework of the Cluster of Excellence MATISSE led by Sorbonne Universités.

Notes

The authors declare no competing financial interest.

ACKNOWLEDGMENT

Funding of KW PhD by China Scolarship Council and Cluster of Excellence MATISSE is acknowledged. We thank Dr F. Le Grand (Institut de Myologie) for fruitful discussion on biological experiments and Dr M. Boissière (Université de Cergy-Pontoise) for his help in confocal microscopy experiments.

REFERENCES

(1) Kattuka, S.; Byrnes, J. R.; Wolberg, A. S. Fibrinogen and Fibrin in Hemostasis and Thrombosis. *Arterioscler. Thromb. Vasc. Biol*. **2017**, *37*, e13-e21.

(2) Laki K. The polymerization of proteins: the action of thrombin on fibrinogen. *J. Biol. Chem.* **1951**, *222*, 815–821.

(3) Ferry, J. D. The mechanism of polymerization of fibrinogen. *Proc. Natl Acad. Sci. USA* **1952**, *38*, 566-569.

(4) Scheraga, H. A. The thrombin-fibrinogen interaction. *Biophys. Chem*. **2004**, *112*, 117-130.

(5) Blombäck, B.; Hessel, B.; Hogg, D.; Therkildsen, L. A two-step fibrinogen-fibrin transition in blood coagulation. *Nature* **1978**, *275*, 501-505.

(6) Blombäck, B.; Bark, N. Fibrinopeptides and fibrin gel structure. *Biophys. Chem*. **2004**, *112*, 147-151.

(7) Higgins, D. L.; Lewis, S. D.; Shafer, J.A. Steady state kinetic parameter for the thrombin-catalyzed conversion of human fibrinogen to fibrin. *J. Biol. Chem*. **1983**, *258*, 9276-9282

(8) Wolberg, A.S. Thrombin generation and fibrin clot structure. *Blood Rev*. **2007**, *21*, 131-142.

(9) Gaffney, P. J.; Whitaker, A. N. Fibrin crosslinks and lysis rates. *Thromb. Res*. **1979**, *14*, 85-94.

(10) Ferry, J. D.; Morrison, P. R. Preparation and Properties of Serum and Plasma Proteins. VIII. The Conversion of Human Fibrinogen to Fibrin under Various Conditions. *J. Am. Chem. Soc*. **1947**, *69*, 388-400.

(11) Shulman, S. The effects of certain ions and neutral molecules on the conversion of fibrinogen to fibrin. *Discuss. Faraday Soc*. **1953**, *13*, 109-115

(12) Blombäck, B.; Okada, M. Fibrin gel structure and clotting time. *Thromb. Res*. **1982**, *25*, 51-70.

(13) Mathur, A.; Schlapkohl, W. A.; Di Cera, E. Thrombin-fibrinogen interaction: pH dependence and effects of the slow-fast transition. *Biochemistry* **1993**, *32*, 7568-7573.

(14) Blombäck, B.; Carlsson, K.; Fatah, K.; Hessel, B.; Procyk, R. Fibrin in human plasma: gel architectures governed by rate and nature of fibrinogen activation. *Thromb. Res*. **1994**, *75*, 521-538.

(15) Kurniawan, N. A.; van Kempen, T. H. S.; Sonneveld, S.; Rosalina, T. T.; Vos, B. E.; Jansen, K. A.; Peters, G. W. M.; van de Vosse, F. N.; Koenderink, G. H. Buffers Strongly Modulate Fibrin Self-Assembly into Fibrous Networks. *Langmuir* **2017**, *33*, 6342-6352.

(16) Cornwell, K. G.; Pins, G. D. Discrete crosslinked fibrin microthread scaffolds for tissue regeneration. *J. Biomed. Mater. Res. A* **2007**, *82A*, 104–112.

(17) Gorodetsky, R. The use of fibrin-based matrices and fibrin microbeads (FMB) for cell-based tissue regeneration. *Expert Opin. Biol. Ther*. **2008**, *8*,1831-1846.

(18) Rejinold, N.S.; Muthunarayanan, M.; Deepa, N.; Chennazhi, K. P.; Nair, S. V.; Jayakumar, R. Development of novel fibrinogen nanoparticles by two-step co-acervation method. *Int J Biol Macromol*. **2010**, *47*, 37–43.

(19) Abelseth, E.; Abelseth, L.; De la Vage, L.; Beyer, S. T.; Wadsworth, S. J.; Willerth, S. M. 3D Printing of Neural Tissues Derived from Human Induced Pluripotent Stem Cells Using a Fibrin-Based Bioink. *ACS Biomater. Sci. Eng*. **2019**, *5*, 234-243.

(20) Ahmed, T. A. E.; Dare, E. V; Hincke, M. Fibrin: A Versatile Scaffold for Tissue Engineering Applications. *Tissue Eng. Part B Rev*. **2008**, *14*, 199–215.

(21) Janmey, P. A.; Winer, J. P.; Weisel, J. W. Fibrin gels and their clinical and bioengineering applications. *J. R. Soc. Interface* **2009**, *6*, 1–10.

(22) Fusseneger, M.; Meinhart, J.; Höbling, W.; Kullich, W.; Funk, S.; Bernatzky, G. Stabilized Autologous Fibrin-Chondrocyte Constructs for Cartilage Repair *in Vivo*. *Ann. Plast. Surg.* **2003**, *51*, 493-498.

(23) Long, J. L.; Tranquillo, R. T. Elastic fiber production in cardiovascular tissue-equivalents. *Matrix Biol*. **2003**, *22*, 339-350.

(24) Willerth, S. M.; Arendas, K. J.; Gottlien, D. I.; Sakiyama-Elbert, S. E. Optimization of fibrin scaffolds for differentiation of murine embryonic stem cells into neural lineage cells. *Biomaterials* **2006**, *27*, 5990-6003.

(25) Oage, R. L.; Malcuit, C.; Vilner, L.; Vojtic, I.; Shaw, S.; Hedblom, E.; Hu, J.; Pins, G. D.; Rolle, M. W.; Dominko, T. Restoration of Skeletal Muscle Defects with Adult Human Cells Delivered on Fibrin Microthreads. *Tissue Engin. Part A* **2011**, *17*, 2629-2640.

(26) Spotnitz, W. D. Fibrin Sealant: The Only Approved Hemostat, Sealant, and Adhesive—a Laboratory and Clinical Perspective. *ISRN Surg*. **2014**, *2014*, 203943.

(27) Brown, A. E. X., Litvinov, R. I.; Discher, D. E.; Purohit, P. K.; Weisel, J. W. Multiscale Mechanics of Fibrin Polymer: Gel Stretching with Protein Unfolding and Loss of Water. *Science* **2009**, *325*, 741-744.

(28) Piechocka, I. K.; Bacabac, R. G.; Potters, M.; MacKintosh, F. C.; Koenderink, G. H. Structural Hierarchy Governs Fibrin Gel Mechanics. *Biophys. J.* **2010**, 98, 2281-2289.

(29) Moreno-Arotzena, O.; Meier, J. G.; del Amon, C.; Garcia-Aznar, J. M. Characterization of Fibrin and Collagen Gels for Engineering Wound Healing Models. *Materials* **2015**, *8*, 1636-1651.

(30) Breen, A.; O'Brien, T.; Pandit, A. Fibrin as a delivery system for therapeutic drugs and biomolecules. *Tissue Eng. Part B Rev*. **2009**, *15*, 201–214.

(31) Brownlee, M.; Vlassara, Cerami, A. Nonenzymatic Glycosylation Reduces the Susceptibility of Fibrin to Degradation by Plasmin. *Diabetes 1983*, **32**, 680-684.

(32) Procyk, R.; King, R. G. The elastic modulus of fibrin clots and fibrinogen gels: The effect of fibronectin and dithiothreitol. *Biopolymers* **1990**, *29*, 559-565.

(33) Duong, H.; Wu, B.; Tawill, B. Modulation of 3D Fibrin Matrix Stiffness by Intrinsic Fibrinogen-Thrombin Compositions and by Extrinsic Celluar Activity. *Tissue Eng. Part A* **2009**, *15*, 1865-1876.

(34) Bidault, L.; Deneufchatel, M.; Vancaeyzeele, C.; Fichet, O.; Larreta-Garde, V. Self-Supported Fibrin-Polyvinyl Alcohol Interpenetrating Polymer Networks: An Easily Handled and Rehydratable Biomaterial. *Biomacromolecules* **2013**, *14*, 3870-3879.

(35) Brown, E. E.; Hu, D.; Lail, N. A.; Zhang, X. Potential of Nanocrystalline Cellulose-Fibrin Nanocomposites for Artificial Vascular Graft Applications. *Biomacromolecules* **2013**, *14*, 1063-1071.

(36) Brown, A. C.; Barker, T. H. Fibrin-based biomaterials: Modulation of macroscopic properties through rational design at the molecular level. *Acta Biomater*. **2014**, *10*, 1502-1514.

(37) Beaumont, M.; Bacher, M.; Opietnik, M.; Gindl-Altmutter, WW.; Potthast, A.; Rosenau, T. A General Aqueous Silanization Protocol to Introduce Vinyl, Mercapto or Azido Functionalities onto Cellulose Fibers and Nanocelluloses. *Molecules* **2018**, *23*, 1427.

(38) Mahony, O.; Tsigkou, O.; Ionescu, C.; Minelli, C.; Ling, L.; Hanly, R.; Smith, M. E.; Stevens, M. M.; Jones J. R. Silica-Gelatin Hybrids with Tailorable Degradation and Mechanical Properties for Tissue Regeneration. *Adv. Funct. Mater*. **2010**, *20*, 3808.

(39) Hoyosa, K.; Ohtsuki, C.; Kawai, T.; Kamitakahara, M. Ogata, S.; Miyazaki, T.; Tanihara, M. A novel covalently crosslinked gel of alginate and silane with the ability to form bone-like apatite. *J. Biomed. Mater. Res. A* **2004**, *71*, 596-601.

(40) Connell, L. S.; Romer, F.; Suarez, M.; Valliant, E. M.; Rhang, Z.; Lee, P. D. ; Smith, M. E.; Hanna, J. V.; Jones, J. R. Chemical characterisation and fabrication of chitosan–silica hybrid scaffolds with 3-glycidoxypropyl trimethoxysilane. *J. Mater. Chem. B* **2014**, *2*, 668-680.

(41) Bourges, X.; Weiss, P.; Daculsi, G.; Legeay, G. Synthesis and general properties of silated-hydroxypropyl methylcellulose in prospect of biomedical use. *Adv. Colloid Interface Sci*. **2003**, *99*, 215-228.

(42) Guillory, X.; Tessier, A.; Gratien, G.-O.; Weiss, P.; Colliec-Jouault, S. ; Dubreuil, D. ; Lebreton, J. ; Le Bideau, J. Glycidyl alkoxysilane reactivities towards simple nucleophiles in organic media for improved molecular structure definition in hybrid materials. *RSC Adv*. **2016**, *6*, 74087-74099.

(43) Connell, L. S.; Gabrielli, L.; Mahony, O.; Russo, L.; Cipolla, L.; Jones, J. R. Functionalizing natural polymers with alkoxysilane coupling agents: reacting 3-glycidoxypropyl trimethoxysilane with poly(γ-glutamic acid) and gelatin. *Polym. Chem*. **2017**, *8*, 1095-1103.

(44) Secundo, F. Conformational changes of enzymes upon immobilisation. *Chem. Soc. Rev*. **2013**, *42*, 6250-6261.

(45) Livage, J.; Coradin, T.; Roux, C. Encapsulation of biomomecules in silica gels. *J. Phys. Cond. Matter* **2001**, *12*, R673-R691.

(46) Fernandes, F. M.; Coradin, T.; Aimé, C. Self-assembly in Biosilicification and Biotemplated Silica Materials. *Nanomaterials* **2014**, *4*, 792-812.

(47) Heinemann, S.; Coradin, T.; Desimone, M. F. Bio-inspired silica–collagen materials: applications and perspectives in the medical field. *Biomater. Sci*. **2013**, *1*, 688-702.

(48) Eglin, D.; Shafran, K. L.; Coradin, T.; Perry, C. C. Comparative study of the influence of several silica precursors on collagen self-assembly and of collagen on 'Si' speciation and condensation. *J. Mater. Chem*. **2006**, *16*, 4220-4230.

(49) Chen, Y.; Mao, H.; Zhang, X.; Gong, Y.; Zhao, N. Thermal conformational changes of bovine fibrinogen by differential scanning calorimetry and circular dichroism. *Int. J. Biol. Macromol*. **1999**, *26*, 129-134.

(50) Johnson Jr., C. W. Protein Secondary Structure and Circular Dichroism: A Practical Guide. *Proteins: Struct., Funct., Genet*. **1990**, *7*, 205-214.

(51) Donovan, J. W.; Mihalyi, E. Conformation of fibrinogen: calorimetric evidence for a three-nodular structure. *Proc. Natl Acad. Sci. USA* **1974**, *71*, 4125-4128.

(52) Privalov, P. L.; Medved, L. V. Domains in the Fibrinogen Molecule. *J. Mol. Biol*. **1982**, *159*, 665-683.

(53) Medved, L.; Litvinovich, S.; Ugarova, T.; Matsuka, Y.; Ingham, K. Domain structure and functional activity of the recombinant human fibrinogen gamma-module (gamma148-411). *Biochemistry* **1997**, *36*, 4685-4693.

(54) Wasilewska, M.; Adamczyk, Z.; Jachimska, B. Structure of Fibrinogen in Electrolyte Solutions Derived from Dynamic Light Scattering (DLS) and Viscosity Measurements *Langmuir*, **2009**, *25*, 3698–3704.

(55) Otzen, D. Protein-surfactant interactions: A tale of many states. *Biochim. Biophys. Acta* **2011**, *1814*, 562-591.

(56) Otzen, D. E.; Sehgal, P.; Westh, P. α-Lactalbumin is unfolded by all classes of detergents but with different mechanisms, *J. Coll. Interface Sci*. **2009**, *329*, 273–283.

(57) Ross, J. J.; Tranquillo, R. T. ECM gene expression correlates with in vitro tissue growth and development in fibrin gel remodeled by neonatal smooth muscle cells. *Matrix Biol*. **2003**, *22*, 477-490.